Performance prediction methodology and analysis of a variable pitch fan turbofan engine

Aleksandar Joksimovic, Sébastien Duplaa, Yannick Bousquet, Nicolas Tantot

Performance prediction methodology and analysis of a variable pitch fan turbofan engine

A. Joksimovic[a] and S. Duplaa[b] and Y. Bousquet[c]
ISAE Supaero, Toulouse, 31400

N. Tantot[d]
Safran Aircraft Engines, Moissy-Cramayel, 77550

The objective of this paper is development and application of a methodology for preliminary analysis of variable pitch fan (VPF), both as a separate component and as a module integrated into a short-medium range geared turbofan engine developed within European FP7 project ENOVAL. For this purpose, a high bypass ratio two spool geared turbofan engine model was constructed in software PROOSIS. A VPF performance modeling methodology was then developed using 3D steady RANS CFD produced fan maps as baseline; the CFD maps characterized five discrete fan pitch angle settings. In order to represent those maps in PROOSIS and add the pitch angle as a degree of freedom, they were transformed into the Map Fitting Tool (MFT) reference frame. Once the complete VPF turbofan model was in place, engine mission optimization experiments were carried out. The resulting performance is characterized by a good capability to control the fan surge margin, without degrading the engine fuel consumption. This paper represents a new contribution on the topic firstly by coupling a 0D engine performance code with a 3D RANS calculation, and then by introducing the concept of MFT maps with an additional degree of freedom as the interface between the two.

[a] Researcher, Aerodynamics, Energetics and Propulsion Department, Aleksandar.joksimovic@isae.fr
[b] Associate Professor, Researcher, Aerodynamics, Energetics and Propulsion Department, Sebastien.Duplaa@isae.fr
[c] Associate Professor, Researcher, Aerodynamics, Energetics and Propulsion Department, Yannick.Bousquet@isae.fr
[d] Engineer, Aerodynamics Department, Nicolas.Tantot@safran.com

Nomenclature

BPR = Bypass ratio

CFD = Computational Fluid Dynamics

MFT = Map Fitting tool

N_c = Corrected rotational speed

OPR = Overall pressure ratio

PR = Pressure ratio

SFC = Specific fuel consumption

SM = Surge margin

SM_N = Surge margin at constant rotational regime

TRL = Technology readiness level

VPF = Variable Pith Fan

Wc = Corrected mass flow

π = Pressure ratio

η = Efficiency

I. Introduction

When talking about the fan module in particular, recent tendencies in the civilian aeronautical propulsion industry could be looked upon from two perspectives. Aiming at reducing engine thrust specific fuel consumption, the first and foremost tendency is to go towards higher bypass ratio engines, with the so called Ultra High Bypass Ratio (UHBR) engines, characterised by bypass ratio of up to 20. The reason for this can be deduced from the basic turbofan analytical considerations which show that the engine SFC decreases with increasing bypass airflow. Simultaneously, for a higher propulsive efficiency of the engine, it is of interest to reduce the bypass ejection speed, or consecutively the fan pressure ratio (PR) [1]. Another typical trend in the European research to consider here is study of variable thermodynamic cycles in order to adapt the engine behaviour to various operating points during the mission. For this purpose, devices that enable variable geometry

and thermodynamics have been studied in the recent years, for example within European project E-BREAK [2]. The two outlined tendencies cross over in a European FP7 project ENOVAL task which deals with low pressure system of the civilian engines. In this context, the task investigated variable pitch fan (VPF) module as means to control engine operability i.e. fan surge margin. It was shown that the variable pitch fan could be used for manipulating the relative position between the operating line and the fan surge line. The left part of Fig.1 illustrates the displacement of the low PR fan operating line towards the surge zone as a consequence of decrease in Mach number (e.g. at takeoff). To remedy for this behaviour and increase the surge margin, the map itself can be displaced relative to the operating line by means of a variable pitch fan (Fig.1, right) [3]. This comes as an attractive feature if the previously mentioned trend to reduce fan PR is taken into account. Reference [3] shows that low PR fans have poor stability at lower rotational regimes at low Mach numbers, as the operating line moves away from the critical line (which indicates the limit of choked flow); this applies at low Mach number flight cases such as takeoff and landing (Fig.1). The same author shows that a solution to avoid this problem would be a fan with variable pitch blades, which would allow a possibility to actively control the fan SM - either to reduce it if it is unnecessarily high in favour of a potential efficiency benefit, or to increase it in situations of particular relevance in terms of safety, e.g. takeoff or landing with cross wind.

Different VPF turbofan technologies were produced throughout the years. VPF equipped turbofan called Astafan, which aimed at improving the fuel efficiency by running at constant rotational speed was developed by Turbomeca. Its first prototype test run was in 1969, it was being developed until the late 1980s, but it was ultimately never produced commercially. Early 1990s saw the development of Advanced Ducted Propulsor (ADP) by Pratt Whitney and NASA. As opposed to Astafan, ADP mounted a VPF on a turbofan for noise reduction purposes [4]. Most recently, Rolls Royce announced development of a VPF equipped turbofan called UltraFan, possibly entering into service by 2025. According to Haselbach et al. [5], UltraFan VPF module would enable optimal low pressure fan operability, as well as the elimination of the need for a thrust reverser.

Despite the idea of a VPF turbofan being far from new, no references were found in the literature on modelling such a technology at a complete engine level, as opposed to the fixed fan geometry

engines, which is commonplace. It was therefore relevant in the first place to identify fixed fan calculation methods that could be extended to accommodate the additional degree of freedom (fan pitch). When fan performance is discussed, standard methods to produce the data are either experimental or numerical (CFD). Given that the current fan/engine technology is at a low TRL and 3D steady-RANS approach was identified as sufficient for producing fan performance data. In order to integrate this fan behaviour into a complete engine cycle, software PROOSIS was used. PROOSIS is a European-developed object oriented software dedicated to turbomachinery system modelling, developed within EU project VIVACE. For more details on PROOSIS, see A. Alexiou and A. Tsalavoutas [6]. In terms of fan, compressor and turbine modelling, PROOSIS default components are only capable of representing the configurations without variable geometry, through generic component maps. Zarati et al. [2] used PROOSIS to explore variable cycles enabled by variable nozzle areas, but no work that dealt with variable turbomachinery rotor geometry was found. PROOSIS users are enabled to insert their own component maps. The performance map of turbomachinery components such as fan can be represented in a frame of reference based on work and loss coefficients, rather than the standard one ($\pi - Wc - \eta - Nc$). This frame of reference, called MFT (Map Fitting Tool), was developed by NASA, and presented in [7]. MFT came forward as relevant because it is extensively used in PROOSIS components; a presentation is available in Sethi et al. [8]. Moreover, since MFT is about an analytical representation of the maps, expressed by a series of physical parameters, it can be used first of all to complete a map by interpolation, and where needed extrapolate performance to very high or very low speed regimes. With this capability, MFT becomes an obvious choice for being extended by the additional degree of freedom (pitch angle), in order to provide a modeling capability.

The objective of the study is twofold, and it is reflected directly through the structure of this paper. The primary objective is to develop a comprehensive engine performance simulation platform adapted for analysis of a VPF equipped turbofan; this will be presented in Section II of this paper. For this purpose, it was envisaged to develop a PROOSIS model (subsection II A) whose input on VPF performance would come from dedicated CFD studies (subsection II B). Subsection II C will introduce the "MFT" reference frame for the fan map, which allows for integrating the

CFD results into the engine system modelling software. The secondary objective is to apply the developed methodology along a typical turbofan mission in order to validate the platform operation and to obtain a first idea of how VPF impacts the fan SM operability and fuel performance of the current engine. Section III contains the description and setup of the performed studies; it is followed by sections on discussion of the presented elements, and a conclusion. This paper represents a new contribution on the topic of variable geometry turbofan engine performance analysis firstly by coupling a 0D engine performance code with a 3D RANS calculation, and then by introducing the concept of MFT maps with an additional degree of freedom (pitch angle) as the interface between the two.

II. Performance prediction methodology

A. Turbofan Engine Cycle Modelling in PROOSIS

The engine selected to be equipped with a VPF module was a short-medium range geared turbofan, designed to power an A320-type aircraft. In order to simulate the engine cycle, system modelling software PROOSIS [6] was used. The baseline cycle specifications, that is, for the cycle with fixed geometry fan, were provided for three operating points (Takeoff, Top of Climb and Start of Cruise) by Safran Aircraft Engines (Table 1). Given that the high pressure and low pressure core performance maps were a priori unknown, the essential part of the cycle design procedure was the map scaling. In order to calculate the map scalars, a multipoint design procedure was carried out [9]. The merit of multipoint design is the capability to take into account constraints that characterize different flight points defined by the user. As a result, the obtained map design (i.e. map scalars) is still unique; however, as opposed to the single point design, it is optimized for all the defined mission points. For the current case, three mission points were used. They were defined, along with their constraints, as follows:

- Takeoff: Maximum thrust (turbine entry temperature) condition;
- Top of Climb: Low pressure system optimization, mass flow condition;
- Cruise: Efficiency and SFC optimization condition.

The engine schematic constructed for setting up the reference cycle is presented in Fig.2. The

engine architecture consists of a high pressure core and a low pressure core linked to the fan by means of a gearbox. All the cooling air for the high pressure and low pressure turbine is taken at the high pressure compressor level. The core and the bypass flows are unmixed, i.e. each flow leaves the engine through a separate nozzle. As previously explained, performance of all the turbomachinery modules of this engine is described by scaling generic component maps in order to match the desired engine design points. This is not the case for the VPF module, because despite having all the necessary capabilities available (e.g. steady, transient, mission analysis) - the crucial drawback of PROOSIS for this project was its lack of capability to represent variable geometry turbomachinery. For this reason, it was necessary to find a way to extend the default PROOSIS component functions in order to take into account the additional degree of freedom of the fan rotor pitch angle. If Reynolds number and γ effects are neglected, compressor performance variables, i.e. performance map, are a function of compressor geometry design only [1]. For this reason, the next step in the VPF modeling was to produce a series of fan performance maps for discrete rotor pitch angles, and at a later phase attempt to reintroduce thus described fan performance into PROOSIS for complete engine analysis.

B. Fan Performance : CFD Maps

For purpose of this task, Safran Aircraft Engines provided a complete VPF stage description. Computations on this geometry were performed using the commercial code NUMECA FINE/Turbo. It solves the steady three dimensional Reynolds Averaged Navier-Stokes equations based on a cell centered finite volume approach on structured grids. All the numerical parameters mentioned below have been set according to previous study [10] that was performed on a similar axial fan and which showed good agreement between experimental measurements and numerical data. The spatial discretization was a central scheme with a Jameson [11] type dissipation using 2nd and 4th order derivatives of the conservative variables. Time integration was performed with an explicit four-stage Runge-Kutta scheme. Conventional techniques as multigrid method, local time step, smooth residual stepping were used to speed up the convergence of the simulations. The turbulence model used for performing the simulations is the single equation model Spalart-Allmaras [12].

The numerical domain consisted of an inlet region, spinner, rotor, outlet guide vane, and the two

exit domains (core and bypass). The Fig.3 represents a meridional view of the calculation domain. The distance between the inlet of the calculation domain and the inlet of the spinner is equal to two rotor blade chords. The structured grid was created with Autogrid V5 and is discretized using H and O topologies. The size of the first cell was set to $1\mu m$ and lead to $y^+ < 1$ near wall regions to allow a good description of the viscous effects and turbulent gradients. The domain point distribution and number of nodes are summarized in Table 2.

To reduce computational cost, only one blade passage per blade row was taken into account in the numerical domain. The interface between the rotor and the stator is treated with the classic mixing plane approach. Five chosen pitch configurations have been calculated : -10^o, -5^o, 0^o, $+5^o$ and $+10^o$. All the configurations have the same mesh characteristics in terms of number of points distribution. Considering the boundary conditions, the total pressure, the total temperature and the flow angle (axial flow) were prescribed at the domain inlet. At the primary duct outlet, a mass flow value was imposed. This value was constant all over the constant rotation speed but changes with the rotation speed. Considering the outlet boundary condition, the characteristic curve representing the total-to-static pressure ratio of the fan depending on the mass flow may have a positive slope at low mass flow rates. Then, a static pressure condition is not adapted as two solutions with different mass flow rates are possible. To accurately simulate the part of the curve having a positive slope, the bypass outlet boundary condition was modeled using a throttle condition. It means that the outlet static pressure imposed by the solver depends on the mass flow rate. The imposed pressure was prescribed according to the following equation:

$$P_{out} = P_{ref} + \lambda \frac{\dot{m}}{\dot{m_{ref}}} \tag{1}$$

$\dot{m}$ is the mass flow rate at the outlet. The reference pressure P_{ref} was set to 101325 Pa while the reference mass flow ($\dot{m_{ref}}$) was set to $668kg/s$ representing the design operating point mass flow. These values were chosen arbitrarily. This boundary condition permitted simulation of different operating points from choke to stall by simply increasing the value of λ. The blades, hub, and shroud walls were treated with a no slip adiabatic condition. For all five configurations, performance maps were defined with 8 iso-speed lines, ranging from 50% to 105% of the nominal

rotation speed. For each iso-speed line, the outlet boundary condition was modified to simulate the complete operating range from choke to stall. To correctly describe the near stall region, the λ value of the boundary condition would be slightly increased. When the λ value increases, the mass flow of the simulated operating points decreases. When the λ value becomes too high, the simulation does not reach a steady state. It would then be considered that stall region was reached. This method was applied for the 8 iso-speed lines and for the 5 configurations. This set of calculations has provided what was considered to be a complete performance map. The resulting maps for the 5 pitch angles are presented in Fig.4.

The following step is integrating these performance maps into PROOSIS. However, they firstly need to be transformed into the format comprehensible by the software, which is the subject of the next section.

C. Transformation of the Maps: Map Fitting Tool (MFT)

PROOSIS turbomachinery components use two types of maps: the Beta maps, described in standard reference frame, and the MFT maps. For various reasons that will be outlined in the following, MFT was adopted as the frame of reference for the current map, which is why a transformation needed to be carried out prior to integrating the resulting maps into the engine model.

The MFT methodology takes description of the given turbomachine work and loss coefficients as the starting point for defining its reference frame. Namely, for each iso speed of a fan or a compressor, a relationship between the work and loss coefficients can be identified, or equivalently, each iso-speed line of the map can be represented in terms of the work (GH) and loss (GL) coefficients. In that frame of reference, the iso speed line takes a parabolic shape. When presented in this manner, it is clear that each iso-speed line is characterized by work that results in minimal losses. When these minimum loss points are identified for all the speed lines, they give basis for the so called backbone line of the compressor map. In other terms: if the compressor operates along the backbone line, it will be working with minimum losses. Compressor map points are thereby represented in terms of their offset from the backbone line. For more details on the MFT map parameters, and their relation to the standard map parameters, see [7] and [8].

In order to transform the five maps, the following input data were required:

- Fan map operating points given by: rotational speed regime, pressure ratio, corrected mass flow and efficiency (CFD output in this case);
- Fan stage geometry parameters, i.e. characteristic cross section areas and radii;
- Inlet reference conditions, i.e. pressure, temperature, humidity level and heat capacity ratio.

It is of utter importance to have smooth evolutions of all the MFT parameters used in the modeling as a function of the rotational regime. Consistency of the five maps transformation was of utmost importance because the goal was to compile a comprehensive map whose above outlined characteristics would be presented with the additional degree of freedom. The analytic relationship of the MFT parameters is crucial because it enables interpolation and extrapolation of the curves in order to complete a map. Taking into account that CFD calculations of a complete performance map can be time consuming, this sort of capability can be very useful for extending the available operating range of the given component. As shown previously, the five discrete pitch angle maps were spanning from 50% to 105% of the nominal rotational regime with a 5% step between 90% and 105%. In order to accommodate any potentially higher rotational regimes that might occur in the subsequent PROOSIS calculations, this range was extended/extrapolated with two additional speed lines: 110% and 115%. Finally, for the five performance maps obtained numerically, the surge line is defined by taking the maximum pressure ratio of each rotation speed characteristic curve. In other words, even if the characteristic curve has a positive slope at low mass flow rate, this part is not taken into account (see $+10^o$ map in Fig.4). The final variable pitch fan engine modeling procedure, described as an assembly of different previously outlined modeling units, is presented in Fig.5.

III. VPF Performance Analysis

A. Engine Mission

The developed methodology was applied on a mission analysis. In PROOSIS, a mission is constructed using time laws of thrust and flight conditions as input. A typical mission data for the current engine was obtained in the ENOVAL project context. This mission profile is illustrated in Fig.6 with time evolutions of net thrust and flight conditions, nondimensionalised by their respective

values at top of climb (Table 3).

When discussing the engine mission at hand, a particular limitation of the model must be pointed out. While constructing the cycle and exploring its characteristics through parametric studies, it was observed that the obtained cycle could not operate below roughly 80% of the nominal fan rotational regime (Fig.7, left). A possible explanation of this behavior was that the best obtainable high pressure compressor map that could be provided for the purposes of this project (for confidentiality reasons) did not sufficiently match the great rotational speed discrepancy between the low pressure and high pressure core, which characterizes the engine cycle at hand. For this reason, the approach and landing phases had to be omitted from the final simulation, since mission calculations failed at the top of landing, when attempting to reach low rotational regimes on the fan map.

The final baseline mission (baseline being with the fan geometry fixed at 0^o pitch) represented by the fan map operating line is shown in Fig.7 (right). In order to avoid redundancy, the calculated baseline fuel burn will be presented in Table 4, where it will be compared to the fuel burned by the optimised cycles. The part 1 of the table presents the results from the mission calculation where the fan SM was being kept at constant value of 10%, whereas part 2 shows the equivalent results of the SFC optimization study with the condition of fan SM $<$ 10%, for the entire mission.

The corresponding fan surge margin time evolution is given in Fig.8. The surge margin parameter that was considered in this work is the surge margin at constant rotational regime, denoted by SM_N.

As it can be seen in Fig.8, the baseline fan surge margin is characterized by low SM of 7 to 10% at the very early takeoff, and high SM peaking at 15% during climb, which levels out at around 13% during cruise. From this baseline trend, the interest in VPF in terms of fan SM was identified:

- To reduce the unnecessarily high SM_N to a prescribed minimal value;
- To increase SM_N to the same safe minimum during the early takeoff.

B. VPF Optimisation Studies

As mentioned in the modeling section, the second part of development work in PROOSIS consisted of expanding the existing component equations, functions and tables in order to accommodate

the additional variable, fan rotor blade pitch. The principal aspect consisted of assembling a coherent VPF MFT map file, which encompassed all the five individual CFD maps transformed into MFT. The rest of the work would then consist of expanding the PROOSIS interpolation functions to use the pitch as an additional interpolation parameter. Additionally, this enabled construction of optimisation experiments where the fan pitch could be used as a decision variable. Additionally, the optimisation experiments had to be assembled to enable mission optimisations with pitch angle as the decision variable. In practice this was performed by using the existing single point optimisation capability of PROOSIS combined with the mission calculation presented in Fig.7 (right). An illustration of single point optimization done in PROOSIS, with fan pitch as the decision variable, is presented in Fig.9. Due to PROOSIS limitations, a fan map cannot be plotted for a variable pitch case, which is why the $\pi - W$ was plotted separately (Fig.9, far right). The basic outline of the developed mission optimisation experiment is summarized as follows:

- The mission is discretised into given number of points along the time axis, corresponding to the points presented in Fig.6;
- Optimization simulation is then performed sequentially for every mission point;
- Each subsequent point is initialized by the previous point results;
- The mission optimisation results are then extracted as time laws.

In this manner, this study was split in two parts, with their respective objective functions given as follows:

- Part 1: SM_N kept at a constant value of 10%;
- Part 2: Optimization of SFC, with SM_N10% constraint.

In practical terms, the goal of Part 1 was to observe the VPF engine behavior if the SM_N was to be kept at a fixed value (10%) during the whole mission. The goal of Part 2 (Optimization) was to assess how much the engine SFC can be further optimized while not allowing the SM_N to go below 10

IV. Discussion

The relevant results of the two optimizations, compared to the corresponding baseline mission performance are illustrated as a function of mission time in Fig.10, and are discussed in the following. The reader is reminded that the baseline performance was obtained with the CFD fan map at the nominal (0^o) pitch angle. Also note that the mission time on the x-axis in Fig.10 is truncated at $t = 1200s$ to improve the clarity of the visualization. In fact, no significant variation of the presented parameters is observed after this time, which justifies this particular focus on takeoff and climb. For the baseline mission (see Fig.10) where no fan pitch angle variation is considered, the fan SM is higher than 10% except at the early takeoff where its value drops up to 8% (Fig.10b). Part 1 aims at keeping a constant SM value of 10% (Fig.10b), which could mean a reduction of up to 35% relative to the baseline (Fig.10c). To obtain this constant value of SM, the fan pitch angle should be increased up to approx. $+3^o$; on the other hand, at the early takeoff it should be reduced up to -2^o (Fig.10a). All intermediate pitch angle variations take place between these two angle values. Compared with the baseline, the consequence is a small increase of SFC: up to 0.4% during the first 700s (except during early takeoff where SFC can be reduced up to -2%) and up to 0.1% during the rest of the mission. In terms of the fuel burnt during the mission, the consumption increase is negligible. (Tab.4) When it is sought to optimize the SFC with keeping the SM equal to or higher than 10%, the Part 2 (SFC optimization) demonstrates that there exists some improvement space. In fact, Fig.10d shows that the SFC can be largely reduced during the takeoff and climb phases, compared to Part 1. Thus optimized SFC value remains slightly lower than the baseline during the rest of the mission, i.e. from approx. $t = 1000s$, all the way until the mission end at t = 26580s. This minor SFC improvement (in other words, very close to the baseline value) is intuitive, because the baseline cycle is designed in order to operate with optimal SFC during the cruise. Furthermore, when this SFC reduction relative to Part 1 is attained, a re-increase of the fan SM is observed (Fig.10b). One remarks that in this case, where the SFC is optimized, it is possible to remain at a SM value higher than the baseline one during the takeoff (Fig.10b). For this optimization the fan pitch angle varies between -2^o and $+0.5^o$ (Fig.10a). The same way as it had been found in Part 1, the global impact of the Part 2 optimization on the fuel burn is negligible (Tab.4). It is

pointed out that an anomaly was observed in terms of the SFC behavior (Fig.10d), notably between t=50s and t=200s where the fan SM did not change relative to the baseline (Fig.10b), but some degradation of the SFC took place nevertheless. This anomaly is of additional interest since no significant change in fan efficiency was observed during this time period (Fig.10e). The question of how an SFC minimization optimization actually led to its increase remains open for the time being, and will be investigated within a further continuation of this work. Nevertheless, even if it had behaved as one might have expected (no change relative to the baseline, or a slight reduction), it would not have had a major impact on the mission fuel burn reduction, which at this moment is -7.5kg. (Table 4) On the whole, it is observed that the main interest of VPF is the possibility to increase the SM during early takeoff, and during the rest of the mission, it is possible to reduce the SM value if necessary. Although the fan SM can be controlled successfully, the VPF does not seem to be capable of providing a simultaneous improvement in the engine SFC. Simultaneously, this does not come as a disadvantage, because it was also observed that the SM control capability does not have a deteriorating impact on the engine fuel burn.

V. Conclusion

VPF was identified primarily as a candidate to ensure a continuous engine safety for nominal configurations characterized by high engine BPR and low fan PR, which would imply compromised fan surge stability at low Mach numbers. For UHBR engines the fan will generate the majority of the thrust, which is why the necessity for continuous fan stability is essential. From the performed work carried out by means of a methodology that combines system modeling in PROOSIS with CFD calculations, it can be seen that VPF can meet the fan surge margin control necessity, in this particular case illustrated by fixing it at prescribed value of 10% throughout the entire mission. Furthermore, the predicted VPF control seems to imply no penalties in fuel burn (calculated through SFC only), which is an important constraint for the contemporary civilian engine industry, as well as the future developments. For a comprehensive conclusion, it remains yet to be seen how a VPF would impact the safety and fuel performance during the approach and landing phase of the mission, which was not possible to simulate during the current work due to technical limitations. Moreover, at a later phase the presented conclusion on the VPF usefulness in terms of operability and fuel

burn would necessarily have to be compared to other technological aspects that are not discussed here, such as system integration, structural complexity, reliability and maintainability, additional drag and added weight. From the performance and fan stability analysis perspective, further course of action which would solidify and complement the findings presented in this paper should take into account the following few guidelines:

- Ensure that the compressor and turbine high pressure core component maps are well adapted to the engine cycle to be modeled in PROOSIS in order to be able to simulate and analyze the entire engine operating range;
- Since the choice of the fan pitch angle variation range can have an impact on the computation time, the selected fan pitch angle range should be reconsidered. A narrower fan blade pivoting range, between -5Âř and +5Âř seems to be better suited for the purposes of a cycle such as this one.

VI. Acknowledgments

The work presented in this paper was carried out within the framework of European Union project ENOVAL (Engine Module Validator), funded by Seventh Framework Program under Grant Agreement no. 604999. The authors would also like to acknowledge the support provided by Safran Aircraft Engines and Empresarios Agrupados.

[1] Philip G Hill and Carl R Peterson. Mechanics and thermodynamics of propulsion. *Reading, MA, Addison-Wesley Publishing Co., 1992, 764 p.*, 1992.

[2] Khaled Zarati, Sebastien Duplaa, Carbonneau Xavier, and Nicolas Tantot. Engine performance and surge margins optimization by variable nozzle area. *ISABE*, 2015.

[3] Victor Bensimhon. *Fonctionnement hors adaptation des turbomachines*. Masson, 1986.

[4] Richard P Woodward, Lawrence A Bock, Laurence J Heidelberg, and David G Hall. Far-field noise and internal modes from a ducted propeller at simulated aircraft takeoff conditions. 1992.

[5] Frank Haselbach, Alan Newby, and Ric Parker. Concepts & technologies for the next generation of large civil aircraft engines. In *29th Congress of the International Council of the Aeronautical Science, St. Petersburg, Russia*, 2014.

[6] Alexios Alexiou and A Tsalavoutas. Introduction to gas turbine modelling with proosis. *Empresarios Agrupados Internacional (EAI) SA, Madrid Spain*, 2011.

[7] George L Converse and RG Giffin. Extended parametric representation of compressor fans and turbines. volume 1: Cmgen user's manual. 1984.

[8] Vishal Sethi, Georgios Doulgeris, Pericles Pilidis, Alex Nind, Marc Doussinault, Pedro Cobas, and Almudena Rueda. The map fitting tool methodology: gas turbine compressor off-design performance modeling. *Journal of Turbomachinery*, 135(6):061010, 2013.

[9] Jeffrey Scott Schutte. *Simultaneous multi-design point approach to gas turbine on-design cycle analysis for aircraft engines*. Georgia Institute of Technology, 2009.

[10] Guillaume Dufour, Nicolás García Rosa, and Sébastien Duplaa. Validation and flow structure analysis in a turbofan stage at windmill. *Proceedings of the Institution of Mechanical Engineers, Part A: Journal of Power and Energy*, 229(6):571–583, 2015.

[11] A. Jameson. Time dependent calculations using multigrid, with applications to unsteady flows airfoils and wings. *10th AIAA Computational Fluid Dynamics Conference, Paper No.91-1596, Reno, NV, USA*, 1991.

[12] P. R. Spalart and S. R. Allmaras. A one-equation turbulence model for aerodynamic flows. *La Recherche Aérospaciale*, 1:5–21, 1994.

Table 1 Selected performance parameters of the baseline engine cycle

Parameter	Unit	Takeoff	Top of Climb	Start of Cruise
Net Thrust	N	85768	22442	19363
BPR	-	15.9	15.5	16.2
OPR	-	46.1	54.7	50.4

Table 2 Number of points of the fan stage numerical domain

Number of Points	Radial Direction	Axial Direction	Azimuthal Direction
Rotor	141	135	73
Stator	105	169	67
	INLET	ROTOR	STATOR
Total Number of Points	$0.334 * 10^6$	$2.668 * 10^6$	$1.596 * 10^6$

Table 3 Top of climb flight conditions for the current engine mission

	Altitude	Mach Number	Net thrust
Top of Climb	10000m	0.78	22300N

Table 4 Baseline fuel burn compared with the results from the two cases.

Part 1	Baseline	Optimized	Δ[kg]	Δ[%]
Complete Mission	6639.1kg	6639.4kg	+0.3	$+4.5 * 10^{-3}$
Takeoff and Climb	290.0kg	294.8kg	+0.8	+0.27
Part 2	Baseline	Optimized	Δ[kg]	Δ[%]
Complete Mission	6639.1kg	6631.6kg	−7.5	−0.11%
Takeoff and Climb	290.0kg	294.0kg	0	0%

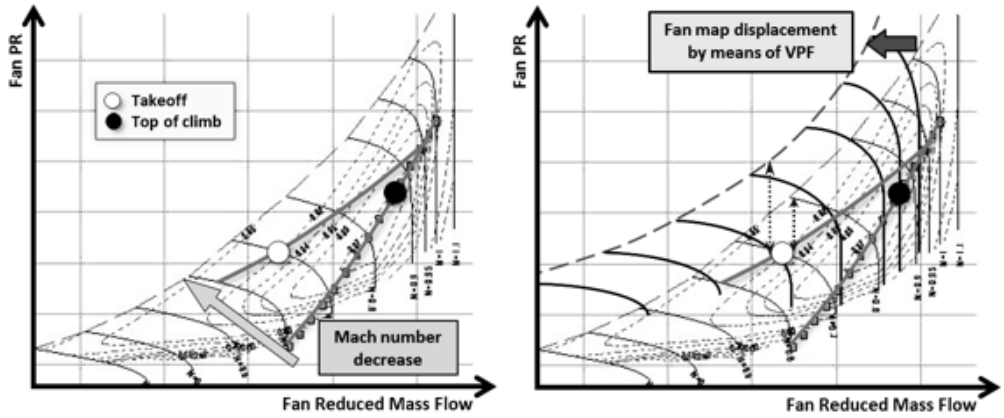

Fig. 1 Fan operating line displacement at low Mach numbers (left); displacement of fan map using VPF (right) [3].

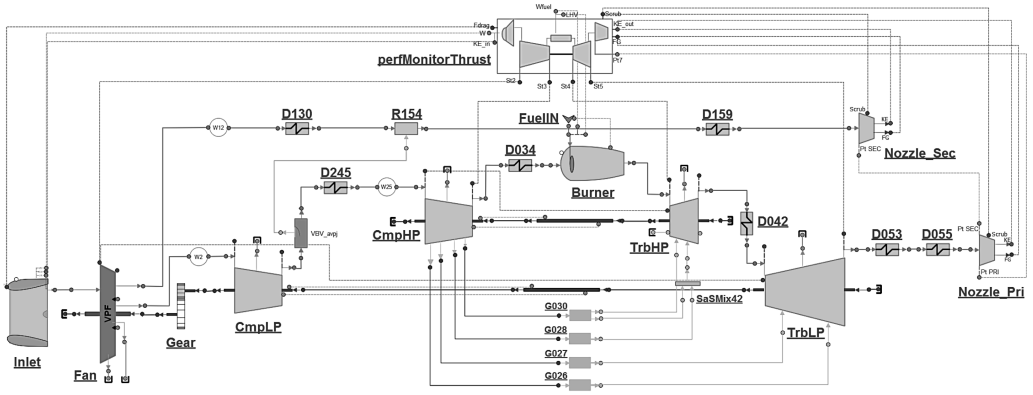

Fig. 2 PROOSIS schematic of a VPF equipped short-medium range geared turbofan

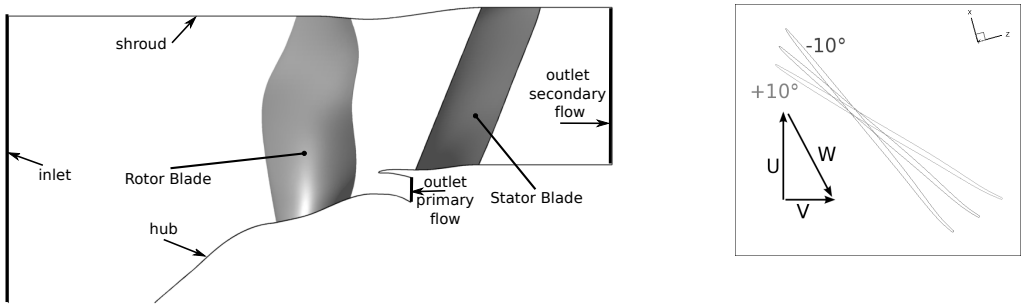

Fig. 3 Meridional view of CFD numerical domain (left); Rotor blade pivoting visualization (right)

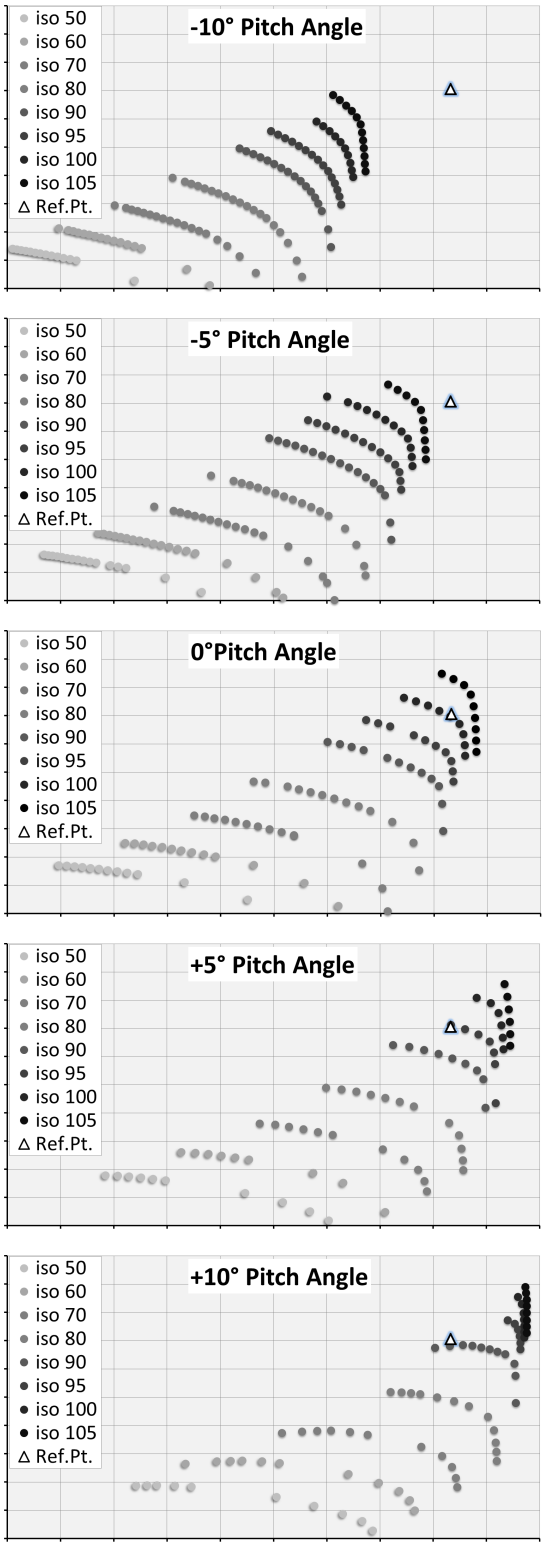

Fig. 4 Resulting CFD maps for the five discrete pitch angles.

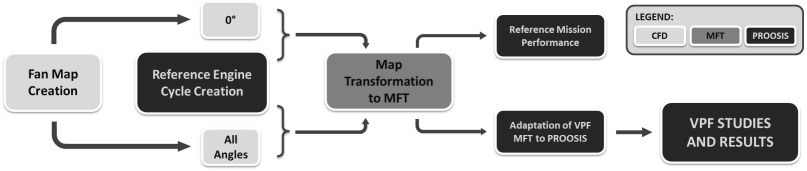

Fig. 5 Flow chart of the system modelling methodology developed to study a VPF turbofan engine.

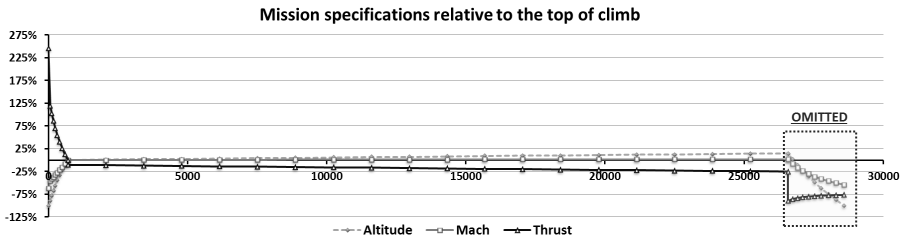

Fig. 6 Engine Mission Specifications.

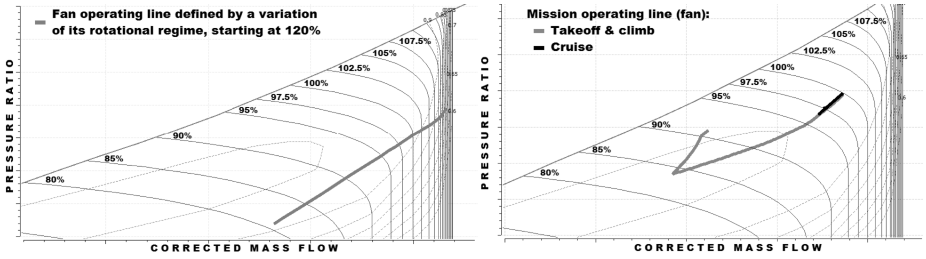

Fig. 7 Fan operating line at top of climb (left), and the mission operating line (right).

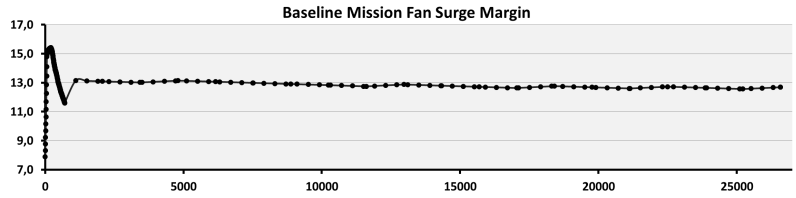

Fig. 8 Baseline fan (fixed pitch) SM in percent, as a function of the mission time.

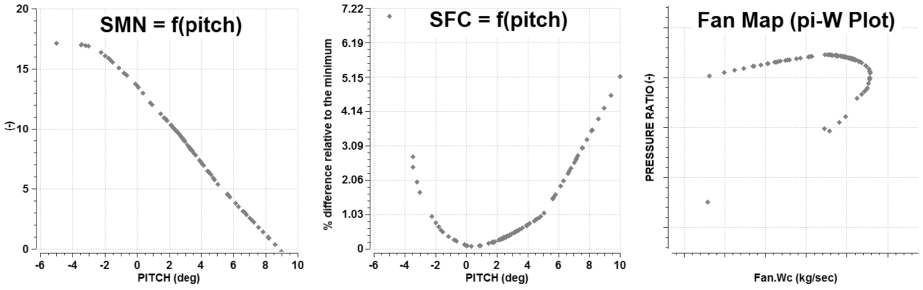

Fig. 9 Single point optimization with fan pitch as decision variable.

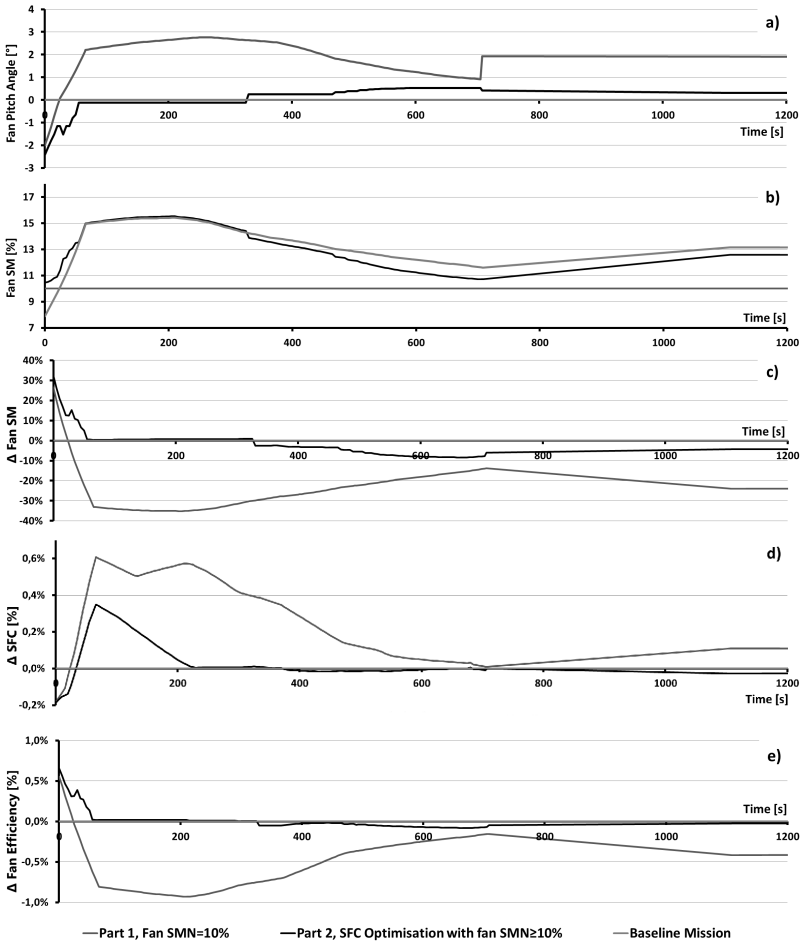

Fig. 10 Parameters time evolution resulting from the two studies, compared to the baseline mission.